Charge transport properties of Ru-complex molecules: the influence of humidity

Atesci, H.

3 Sample preparation and experimental methods

This chapter presents an overview of the methods used to fabricate and characterize the molecular layers of interest, and of the techniques employed to measure and analyze the conductance properties of those layers.

3.1 Introduction

As explained in Section 1.5, our goal is to investigate the charge-transport properties of monolayers of Ru-complex molecules. For this, we take two basic steps. First, well-defined self-assembled monolayers (SAMs) are created on a suitable base material. We choose indium tin oxide (ITO) as a substrate, and phosphonic acid groups as the molecular end groups (the 'glue') connecting to the ITO. After the self-assembly process, the molecules are covalently bound to the ITO, which also serves as a bottom electrode (see Fig. 3.1). Second, we need to contact this self-assembled monolayer (SAM) with a top electrode, so that a voltage bias can be applied between the two electrodes and a current can be produced and recorded. In Chapter 1, we have listed the most common methods with which SAMs are probed. We choose conductive atomic force microscopy (C-AFM) to this end, as it allows us to separate the force feedback process (see Section 3.4) from the conductance experiment. Furthermore, it provides control over several parameters, such as the probe radius, probe material and the force with which we contact the SAM.

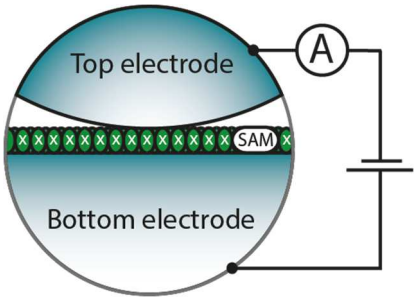

Figure 3.1: Schematic overview of the metal-molecule-metal junction during electron transport measurement.

With these points taken into consideration, let us briefly give an overview of this chapter. We first describe how we grow well-defined molecular layers on conductive ITO substrates. Then, we explain how these SAMs are probed, using C-AFM. Also, we discuss how several important experimental parameters, such as the relative humidity and temperature, are varied, in order to study the transport mechanism in the molecular systems considered. And finally, we will discuss our data analysis methods.

3.2 Sample preparation: molecular self-assembly

Our Ru-complexes have phosphonic acid groups which readily (chemically) bind to indium-tin-oxide (ITO), which is coated on top of glass substrates (purchased from Kuramoto Co., Ltd). The nominal sheet resistance in our case is ≈ 20 Ω/□. For our purposes, the substrates are cut into approximately square 1×1 cm pieces.

To prepare the substrates for molecular self-assembly, we first clean them by the so-called RCA treatment. This essentially means that we heat the samples at 80°C in a mixture consisting of H_2O:H_2O_2:NH_3 in a 5:1:1 volume ratio, for 1 hour. We then wash the substrates with of ultraclean milli-Q water, after which they are further cleaned by Ar-ion etching for 3 minutes (350 eV, 10 mA, 0.3 mbar). After venting the Ar-ion etcher setup, these samples are immediately put into the molecular solution for 30 to 60 minutes, followed by a series of washing steps with milli-Q water (three times). Then, the sample is dried under either Ar or N_2 flow. These molecule-decorated substrates have been used for both the electrochemistry and the C-AFM measurements.

The molecular solution in which the substrates are immersed is a 50 μM Ru-complex aqueous solution prepared by dissolving the Ru-complexes in 5 mL of milli-Q water by adding 3 drops of 25% ammonia solution during ultrasonication. Then the pH of the complex solution is adjusted to pH ≈ 6 by the addition of 0.1% HCl while the pH is monitored by either a pH-meter or pH-paper. The solution is then transferred to a 20 mL volumetric flask and the volume is adjusted by adding milli-Q water. As an example, we dissolve 3.07 mg of **2-Ru-N** in this procedure. A similar protocol is for the other four molecules with varying dissolved mass according to their molecular mass. Note that the recipes described here are the result of a series of optimization steps by Kaliginedi *et al.*(*67*) and Aki-Haga *et al.*(*51*).

3.2 Sample characterization

The Ru-complex molecular layers formed with the method described above have been characterized using an extensive set of methods, such as cyclic voltammetry, X-ray photoelectron spectroscopy (XPS), and atomic force microscopy (AFM) by Kaliginedi *et al.*(*67*), and Aki-Haga *et al.*(*51*). We will highlight the details thereof in the following paragraph. Further information on XPS and AFM characterization can be found in Appendix A.1-A.3.

3.2.1 Cyclic voltammetry

First, we discuss cyclic voltammetry measurements (CVs) on Ru-complex layers. These have been performed by our collaborator V. Kaliginedi. Cyclic voltammetry is an electrochemical characterization technique where the current is measured as a function of the potential of a working electrode in an electrochemical cell. As the potential of the working electrode is increased and decreased in cycles, reduction and oxidation will occur, revealing the electrochemical properties of the analyte. For more information on the subject of cyclic voltammetry, we refer to Ref. (*68*).

Our cyclic voltammogram measurements are done in a Ar atmosphere in a lab-made single compartment glass cell at room temperature in deoxygenated solution, specifically in 0.1M $HClO_4$ in CH_3CN. All cyclic voltammetry measurements are performed employing a lab-made potentiostat under various sweep rates. A platinum wire is used as a counter electrode and Ag/AgCl electrode used as a reference electrode. In Figure 3.2a,b, one sees that **1-Ru-N**, and **1-Ru-Py** show a single reversible redox peak, at different energetic positions. This peak corresponds to the Ru(II) $\Longrightarrow$ Ru(III) redox reaction. The shift between the **1-Ru-N**, and **1-Ru-Py** peaks is a result of the different ligand surroundings that will result in varying degrees of electron withdrawal from the Ru ion, see also Fig. 1.5.

However, when observing the CVs of **2-Ru-N, 2-Ru-C** (Fig. 3.2c,d), one sees two reversible redox peaks corresponding to the sequential oxidation of the two Ru centers present in each molecule: a) Ru(II)–Ru(II) $\Longrightarrow$ Ru(III)–Ru(II), and b) Ru(III)–Ru(II) $\Longrightarrow$ Ru(III)–Ru(III). The reason we see these as separate peaks is due to the electrostatic coupling of the two Ru-centers of these molecules: whenever one Ru-center is charged, the other Ru-center will be electrostatically polarized and hence, a higher potential is required to bring it up to the same charge state as the initial Ru-center. The larger the difference in potential between the two peaks, the stronger is the electrostatic coupling between the two Ru-centers. It can also be noted that **2-Ru-N-dec** (see Fig. 3.2e) even though having two Ru-centers, only yields one reversible redox peak. This is due to two Ru-centers being 'decoupled' (hence the suffix **'dec'**) electrostatically due to the phenyl ring spacer between them.

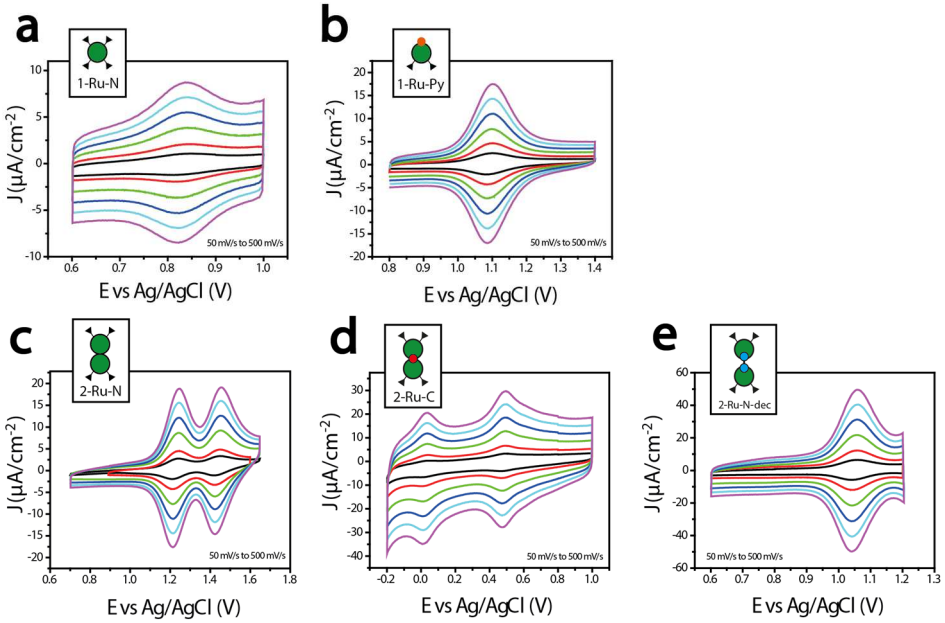

Figure 3.2: Cyclic voltammograms of **1-Ru-N** (a), **1-Ru-Py** (b), **2-Ru-N** (c), **2-Ru-C** (d), **2-Ru-N-dec** (e), monolayers measured in 0.1M $HClO_4$ in CH_3CN with scan rates of 50 (purple line) mV/s up to 500 mV/s (black line). Data provided by V. Kaliginedi.

The stability of the SAM was tested by holding the potential at each peak position for one hour. The CV taken after holding the potential at the peak position (at the left and right peaks) did not show any degradation or decrease in the peak currents. This indicates the electrochemical robustness of the Ru-complex layers. For further details on the electrochemical stability, we refer to one of the following publications(*67*)·(*69*)·(*48*).

In addition to CH_3CN, aqueous electrolytes have also been used. As an example, the cyclic voltammetry of **2-Ru-N** in aqueous electrolyte (0.1M $HClO_4$) is shown in Figure 3.3a. The cyclic voltammograms measured in aqueous electrolyte show only a single redox peak corresponding to the one-electron redox process (i.e., a Ru(II)-Ru(II) $\Longrightarrow$ Ru(III)-Ru(II) couple). The second redox process for a Ru(III)-Ru(II) $\Longrightarrow$ Ru(III)-Ru(III) couple is not accessible in an aqueous electrolyte, unlike the case of non-aqueous CH_3CN (See cyclic voltammetry data given in Fig. 3.2c). Figure 3.3b shows the total integrated charge extracted from the cyclic voltammograms. We find that the current densities of anodic and cathodic peaks show a linear dependence on scan rate, indicating the surface-confined-nature of the redox reaction (in contrast, a non-linear behavior would indicate contributions from sources other than the surface).

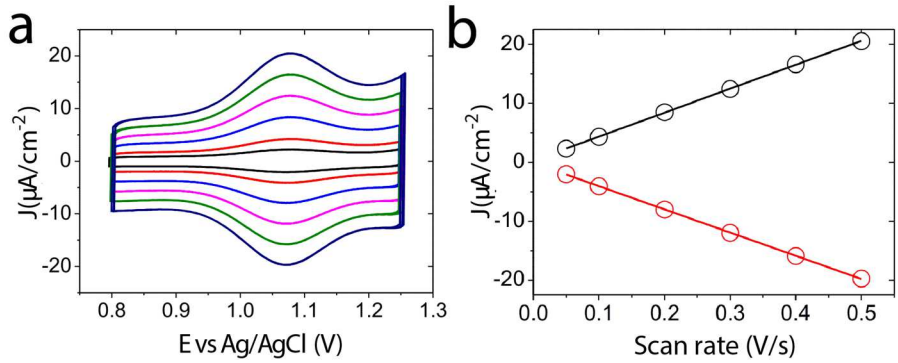

Figure 3.3 : (a) Cyclic voltammograms of **2-Ru-N** monolayers measured in aqueous 0.1M $HClO_4$ with scan rates of 50 - 500 mV/s (dark blue to black, respectively) and (b) the peak current density vs scan rate plot. Data provided by V. Kaliginedi.

3.3 Tip preparation

To probe our SAMs, we use metallic probes as top electrodes in the conductive Atomic Force Microscope setup. The probes are made of solid Pt (type RMN-12PT400B, 0.3 N/m) and have a tip radius of ≈5 nm, making them extremely fragile when in contact. Thus, we sputter coat them with varying thicknesses of different metals (Au, Pt, ITO) to enhance their mechanical robustness. More importantly, this gives us the freedom to experiment with different top electrode chemistries and various tip radii.

We use the scanning electron microscope to determine the tip radii of our tips, as can be seen in Figure 3.4. Unlike traditional silicon-nitride-based AFM probes, these solid Pt probes can be reused if maintained properly and with low forces (such as the force settings used in our work). The tips are always cleaned with an Ar ion beam (350 eV, 10 mA, 0.3 mbar) for 10 seconds before measurement. This ensures a clean tip apex and less measurement noise.

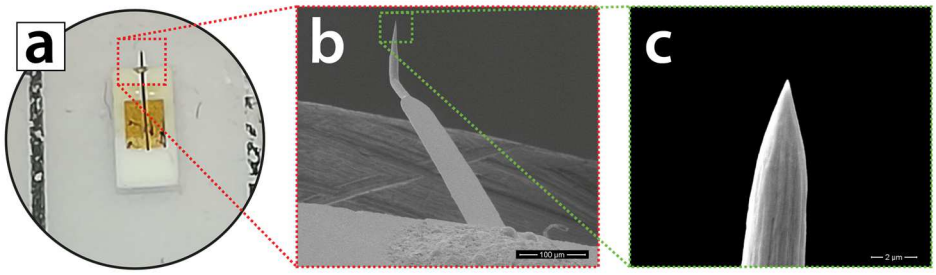

Figure 3.4: Shown in (a) is the macroscopic image of the C-AFM probe used in our work, with a zoom-in revealing the cantilever (b), and a further zoom-in revealing the tip apex (c), which in this case has a tip radius of 50 nm. Images (b) and (c) have been taken by scanning electron microscopy.

3.4 Conductive Atomic Force Microscopy (C-AFM)

Before discussing the actual experimental technique, which is Conductive Atomic Force Microscopy (C-AFM), a brief introduction to Atomic Force Microscopy (AFM) in general, is given. The AFM works by means of a sharp probe attached to a flexible cantilever, which is in contact with the substrate (Fig. 3.5). During scanning, the surface of the substrate will exert position-dependent forces on the cantilever because of its roughness. The cantilever will then bend upward or downward according to the change in height of the surface. To keep the force constant between the tip and the surface, the AFM employs an optical

feedback system where a laser light is reflected off the back of the cantilever and then a mirror, before entering the quadrant photodiode (Figure 3.5a).

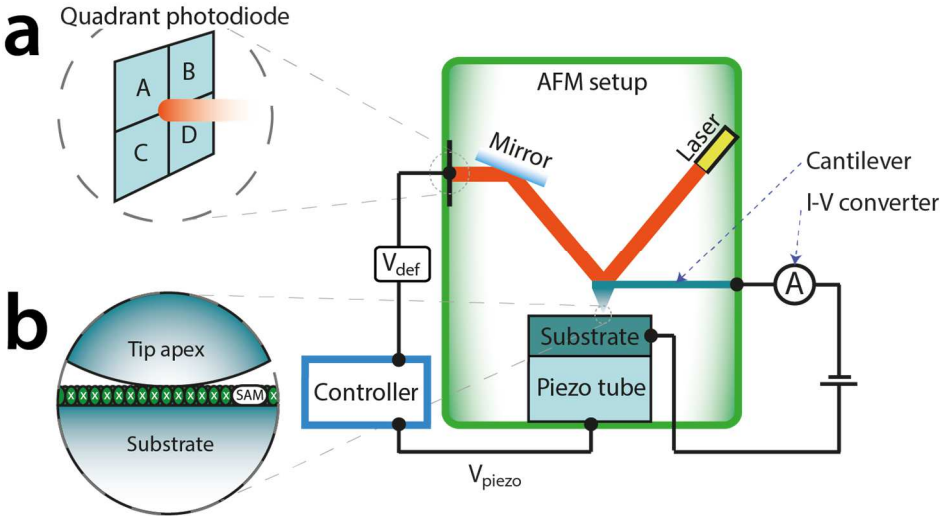

Figure 3.5: Schematic representation of the mechanism of our C-AFM setup with a zoom-in on the quadrant photodiode (a) and the contact of the AFM probe with the substrate coated with a layer of self-assembled molecules (SAM). Current versus voltage measurements can be done once the tip is in contact with the SAM. Note that the tip is grounded in our set-up, i.e. the substrate is at the voltage applied, V.

Height changes in the surface will correspond to a proportional change in cantilever deflection and therefore a vertical signal difference (A+B) - (C+D) on the quadrant photodiode. This diode signal is also referred to as deflection voltage (V_{def}), which is compared to a set reference voltage, the difference of which is multiplied by a feedback gain. The controller then couples this feedback signal to the vertical piezo tube (V_{piezo}), which increases or decreases the sample height to keep the deflection voltage constant. The AFM is run by PI (proportional-integral) control, i.e. the piezo voltage output depends mainly on the proportional gain G_p, and the integral gain G_i (with $V_{def} - V_{set}$ integrated over time t) on top of a constant output value C:

$$V_{piezo} = G_p(V_{def} - V_{set}) + G_i \int_0^t (V_{def} - V_{set})dt + C \qquad (1)$$

The deflection voltage is proportional to the exerted force, which we will use to calibrate the force on the cantilever. Until here, we have only given a short introduction to the "contact mode" AFM, for which the tip is in contact with the surface at all times.

Usually, AFM probes are made of silicon nitride. However, we can add an extra experimental dimension to the AFM by using a metallic probe. Then, we can simultaneously control the force on the substrate while measuring its conductance properties. This is the Conductive-AFM technique that we will be using throughout this dissertation(*70*). In our configuration, the sample is biased and the tip is grounded, while the current is sampled with the I-V converter (Fig 3.5).

3.4.1 Force calibration

We can calibrate the force sensitivity by first doing force-distance ramps on a hard surface, such as sapphire and deriving the slope thereof, which is the deflection constant a in V/m. With the given spring constant of the tips, k = 0.3 N/m, the exerted force on the sample is then given by the following formula:

$$dF = -\frac{k}{a} dV \qquad (2)$$

With our tips, we did many optimizations of the force settings required to get adequate current-voltage (I-V) spectroscopic data without breaking through the molecular layer. We arrived at a force setting of 10.5 nN for the most common tip radius we use, which was 150 nm. For different tip radii we would have to use different forces to prevent exerting too much or too little pressure on the molecular surface. To give us an approximation for the force we need to exert with tips that have varying tip radii (see Ch. 4 and 5), we use the theoretical relationship between the surface contact area and the exerted load by Carpick *et al*.(*71*). From there, we can calculate the average pressure on the surface as a function of the exerted load for different tip radii, the results of which we show in Fig. 3.6.

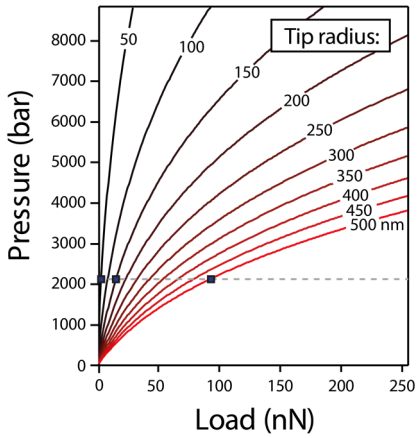

Figure 3.6: Theoretical curves of the pressure on the SAM versus tip load with varying tip radii. The parameters and formulae used for this approximation are derived from the following paper by Carpick *et al*(*71*). Based on this, the exerted pressure as a function of load for different tip radii can be calculated. From the force values extracted from this figure, we performed tip radius dependent measurements while keeping the calculated pressure values constant for all tip radii.

From Fig. 3.6 follows that, for experiments where we want to change the tip radius while requiring to keep the pressure constant (≈ 2 kbar), the exerted force on the sample should change from 2.8 nN to 70 nN for tip radii of 50 and 500 nm, respectively.

3.5 Experimental setup

To prepare the experiments, we place the freshly prepared SAM on the ITO substrate in the sample holder. The conductive cantilever (Fig. 3.7a) is also placed in the tip holder. The zoom-in of cantilever prior to measurement can be seen in Figure 3.7a. The cantilever is connected to the I-V converter with which we read out the conductance data. A complete picture of the setup can be seen in Figure 3.7b.

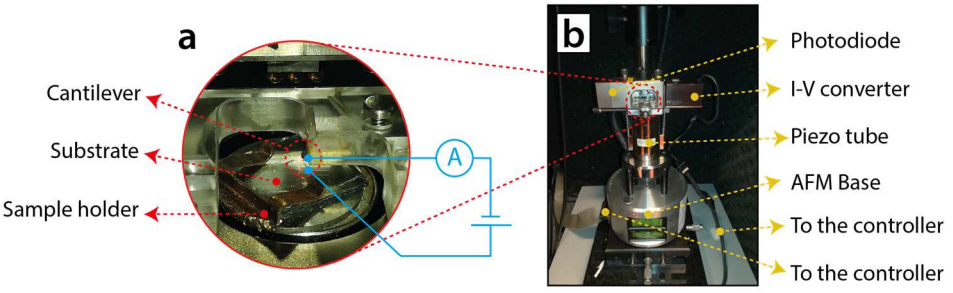

Figure 3.7: Shown in (a) is the detailed zoom-in of the C-AFM probe with the sample prior to measurement with the blue circuit showing the substrate being biased and the tip grounded. In (b) the entire C-AFM setup is shown before putting on the atmospheric hood.

3.5.1 Humidity-dependent measurements

To measure the current-voltage (I-V) characteristics for different values of the relative humidity in the atmosphere, we can purge our system with either dry N_2 or humid N_2 or a mixture of both for variable humidity measurements. For dry N_2 purging, we connect the tube with N_2 flow directly to the atmospheric hood. For humid N_2 purging, we insert the tube with N_2 flow into a glass jar with Milli-Q (ultrapure) water (see Figure 3.8), the exhaust of which is then saturated with water vapor. We then connect this to the atmospheric hood, which is also made into a Faraday cage by covering it in aluminum foil and grounding it. We tested the efficacy of the aforementioned Faraday cage thoroughly before any experiments are made. We also place a hygrometer inside for a direct read out of the humidity. The system is then ready for the final approach of the cantilever, after which the measurements can commence.

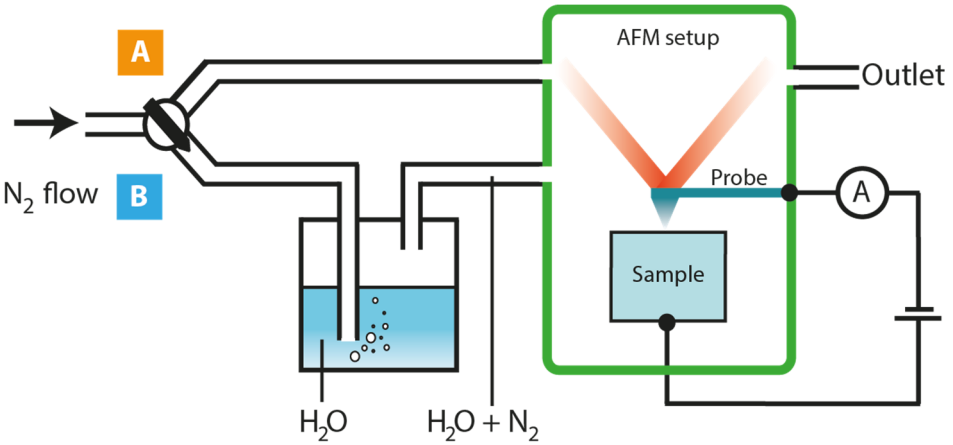

Figure 3.8: Schematic representation of the set-up that that allows one to purge with either dry (A) or humid (B) nitrogen. For humid nitrogen, we purge the system with nitrogen that flows through Milli-Q water. This gas then enters the C-AFM setup seal with an atmospheric hood and a hygrometer with which we can read out the humidity.

3.5.2 Temperature-dependent measurements

In case of temperature-dependent measurements, we can heat the sample holder with a Peltier element (Conrad, QC-32-0.6-1.2) glued underneath it, see Figure 3.9. A bridge will ensure the bias transfer from the bottom disc to the substrate. Extra care should be taken not to short the sample holder with the connections to the power source, that is why we have covered the base of the connections with a plastic casing.

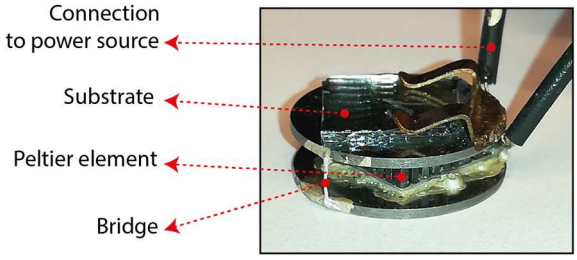

Figure 3.9: Photograph of the sample holder with the Peltier element for temperature-dependent measurements.

3.6 I-V measurements and data analysis

Before each measurement, the chamber is purged thoroughly for 15-30 minutes, during which the tip is out of contact with the sample. Once the desired humidity level is reached, the purging is set at a slower

rate which allows the tip to approach the sample stably so that we can start the acquisition of I-V data. Typically we use a 1-2 V/s sweep rate for I-V measurements with a total of usually between 500 and 2000 sweeps. For highly resistive samples, such as **2-Ru-N** and **2-Ru-C**, we use slower sweep rates, approximately 0.2 V/s, due to the risk of producing hysteretic I-V characteristics from capacitive charging. In this case, we have limited our data size to approximately 100 I-V curves on various locations. The data analysis has been done by a 9 point (35 mV on voltage scale) smoothing of each I-V curve.

Next, the absolute value of all data sets are plotted together on a logarithmic scale, after which we use a 2D histogram to highlight the density of the data sets, as can be seen in an exemplary data set in Figure 3.10a. From the current-voltage data, the 'rectification ratio', RR, can be calculated, which gives us the numerical representation of any rectifying behavior of the I-V characteristic. To obtain the RR, one divides the current at positive bias by the current at negative bias:

$$RR = \left| \frac{I(+V)}{I(-V)} \right| \tag{3}$$

An example of this can be seen in Figure 3.10b. For all 2D histograms, we fit the data set at each voltage bin to a Gaussian fit. The average of the Gaussian fit is then given by a dark blue curve. We then set the error bars to be the standard deviation of the fits. We use this analysis method to provide for a clear overview of the large amounts of data provided in this work.

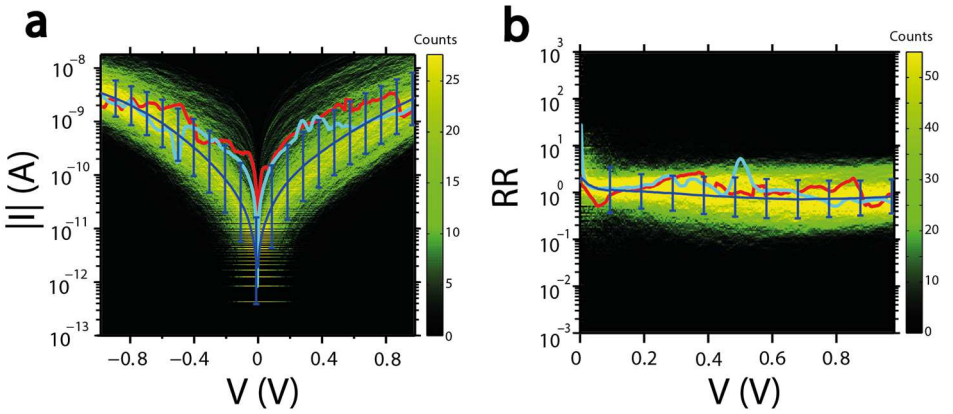

Figure 3.10: (a) An example of a 2D-histograms of logarithmically binned |I|-V characteristics of **1-Ru-N** molecular junctions at ≈5% relative humidity for a 150 nm Au tip with 10.5 nN exerted force. (b) The corresponding 2D-histogram of logarithmically binned RR values against the bias voltage V (b). Two example |I|-V curves with their corresponding RR values are given in the red and turquoise lines. Overlaid in dark blue is the mean of the Gaussian fits at each bias voltage bin. The error bars follow from the standard deviation of the fits.

3.7 Computational details

In the case where we need computational support (beyond the models described in the Theory chapter) to provide further insight into the orbital structure of the Ru-complexes with external stimuli such as water and bias voltage, we use density functional theory (DFT) with the generalized gradient approximation (GGA) and Perdew-Burke-Ernzerhof functional in collaboration with J.M. Thijssen and J.A.C. Gil from the Theoretical Physics group, Delft University. For the transport calculations, the wide band limit is used as well as image-charge correction(*72, 73*). To simulate the solvent, explicit water molecules are included(*74*). A bias voltage is applied to the system by introducing an external uniform electric field along the long axis of the Ru-complex. Geometry optimizations have been made, if necessary at each bias voltage, to include for voltage-dependent effects of the water and ion movements. The non-equilibrium Green's Function theorem is then used to calculate the transmission for every magnitude of the electric field. The current is finally calculated using the Landauer formula (see Ch. 2.3).